CRYSTAL GROWTH & DESIGN

Article

pubs.acs.org/crystal

Crystal Engineering of L-Alanine with L-Leucine Additive using Metal-Assisted and Microwave-Accelerated Evaporative Crystallization

Adeolu Mojibola, Gilles Dongmo-Momo, Muzaffer Mohammed, and Kadir Aslan*

Department of Chemistry, Morgan State University, 1700 East Cold Spring Lane, Baltimore, Maryland 21251 United States

Supporting Information

ABSTRACT: In this work, we demonstrated that the change in the morphology of L-alanine crystals can be controlled with the addition of L-leucine using the metal-assisted and microwave accelerated evaporative crystallization (MA-MAEC) technique. Crystallization experiments, where an increasing stoichiometric amount of L-leucine is added to initial L-alanine solutions, were carried out on circular poly(methyl methacrylate) (PMMA) disks modified with a 21-well capacity silicon isolator and silver nanoparticle films using microwave heating (MA-MAEC) and at room temperature (control experiments). The use of the MA-MAEC technique afforded for the growth of L-alanine crystals with different morphologies up to ~10-fold faster than those grown at room temperature. In addition, the length of L-alanine crystals was systematically increased from ~380 to ~2000 μm using the MA-MAEC technique. Optical microscope images revealed that the shape of L-alanine crystals was changed from tetragonal shape (without L-leucine additive) to more elongated and wire-like structures with the addition of the L-leucine additive. Further characterization of L-alanine crystals was undertaken by Fourier transform infrared (FT-IR) spectroscopy, Raman spectroscopy and powder X-ray diffraction (PXRD) measurements. In order to elucidate the growth mechanism of L-alanine crystals, theoretical simulations of L-alanine's morphology with and without L-leucine additive were carried out using Materials Studio software in conjunction with our experimental data. Theoretical simulations revealed that the growth of L-alanine's {011} and {120} crystal faces were inhibited due to the incorporation of L-leucine into these crystal faces in selected positions.

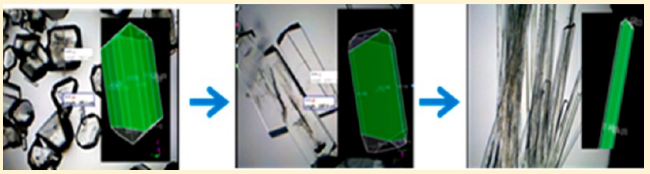

INTRODUCTION

Crystal engineering, which can be broadly described as the design of molecular solids, has gained the interest of researchers worldwide since it affords one the ability to understand the chemical and physical properties of a crystal and the possibility to control and design the way molecules aggregate in the crystalline phase.[1] The control over molecular behavior, such as variations in crystal morphology and the crystal growth kinetics of crystals has promising implications for large scale processing of materials in industry.[2]

Control of crystal morphology can be achieved by the selection of appropriate solvent or tailor-made additives. Additives are present in smaller amounts than the target molecules during the crystallization process, subsequently disrupting the activity of the crystallizing solute in solution. Additives simultaneously interfere with the crystal's growth process via adsorption onto the growing crystal surface.[3] For example, Mirza's group reported on the crystal morphology engineering of erythromycin, a macrolide antibiotic, in which they investigated this compound as a tool for tailoring tableting performance of pharmaceutical solids. Using hydroxypropyl cellulose as an additive, they discovered that the additive improved the compaction properties of the substrate, proving crystal engineering to be a valuable tool for the enhancement of tableting properties of pharmaceutical drugs.[2,4] Doki's research group proposed a new technique based on natural cooling crystallization combined with pulse heating, where a tailor-made additive (i.e., cysteine) was used as a separation agent for the simultaneous crystallization of D-asparagine and L-asparagine. Their results showed that the utilization of a natural cooling crystallization method resulted in a delayed nucleation phase in L-asparagine in the presence of L-cysteine additive, while D-asparagine remained unchanged. They also discovered that the nucleation phase of L-asparagine was more significantly delayed with an increase in the L-cysteine concentration.[5]

The use of hydrophobic amino acids has also attracted major interest in the crystal engineering field primarily due to their ability to create hydrophobic pockets during protein folding.[6] L-Alanine, in particular, has been extensively studied by many crystal engineers due to its structural simplicity and abundance in all proteins.[7] For example, Raj and Kumar have reported their work on the morphology and thermal expansion of nonlinear optically pure and deuterated L-alanine crystals using cooling and seed rotation techniques. They discovered that the morphology of L-alanine crystals grown using both techniques resulted in the same Miller planes; other findings showed that the thermal expansion of deuterated L-alanine is lower than its optically pure counterpart.[8] In addition, one can find several other reports on L-alanine's molecular behavior with the

Received: February 9, 2014
Revised: March 21, 2014
Published: March 21, 2014

dx.doi.org/10.1021/cg500204t | Cryst. Growth Des. 2014, 14, 2494−2501

addition of tailor-made additives in literature. Ballesteros and Hornedo reported on the adsorption effects of hydrophobic and hydrophilic tailor-made additives on L-alanine's growth kinetics and morphology. They discovered that L-alanine grown in the presence of hydrophobic amino acids displayed changes in its growth kinetics and morphology, while the use of hydrophilic amino acids revealed no such changes.[3,4,9,10] Yang's group has also demonstrated the effects of tailor-made additives on L-alanine. In their study, the influence of L-valine on the growth rate of the {011} and {120} faces of L-alanine was reported. The adsorption of L-valine onto the surface of L-alanine was shown to result in a relatively small reduction in the growth of the {011} face, whereas the {120} face's growth rate was significantly reduced.[11] Despite the knowledge gained from these reports, there is still a need for techniques that improve the crystallization process in terms of rapidity and control over the size and morphology of crystals grown, while still providing a detailed knowledge of the characteristics of the amino acid being studied.

In the previous publications from our laboratory, we have demonstrated that the use of the metal-assisted and microwave accelerated evaporative crystallization (MA-MAEC) technique can reduce the complete evaporation time of amino acids and small organic compounds to a fraction of the time compared with the conventional evaporative crystallization method. In this regard, L-alanine,[12] L-glycine,[13] L-arginine,[14] and acetaminophen[15] were crystallized with the combined use of silver modified glass and PMMA platforms[16] and a commercial microwave, in which the crystallization process was reduced from several hours to seconds. In the MA-MAEC technique, silver nanoparticle films (SNFs) serve as selective nucleation sites for the crystal growth of the amino acid due to the interactions of the primary amine of the amino acid and SNFs and as a microwave-transparent medium for the creation of a thermal gradient between the warmer solution and the SNFs that remain at room temperature during microwave heating [note, a more in-depth explanation of the mechanism of the MA-MAEC technique can be accessed through previous publications from our laboratory].[17] Our research group has also studied the crystallization of L-alanine in the presence of L-valine and L-tryptophan additives using the MA-MAEC technique. This study revealed that the incorporation of these additives resulted in an increase in the size, a change in morphology, and an improvement in quality of L-alanine crystals.[16] The use of these additives were based on their similarities to L-alanine in structure and isoelectric points: 5.96 for L-valine; 5.98 for L-tryptophan compared with 6.11 for L-alanine. The results of this study enabled us to extend our analysis of the growth behavior of L-alanine with the incorporation L-leucine as additive. L-Leucine can be considered as a tailor-made additive that also has the ability to modify the crystal morphology of L-alanine.[16]

Subsequently, in this work, we focus our efforts to understanding the effects of L-leucine additive on the crystal structure of L-alanine. The growth of L-alanine crystals both in the absence and in the presence of L-leucine was accelerated with the use of the MA-MAEC technique. The morphology of L-alanine changed from tetragonal to elongated, wire-like structures as the extent of L-leucine additive was increased in the initial amino acid mixture. The wire-like amino acid crystal can be used in applications of nonlinear optics. To gain a better understanding of L-alanine's structural behavior when L-leucine additive is incorporated, theoretical simulations were also employed. Theoretical molecular models of L-alanine crystals with and without L-leucine additive were obtained and compared with L-alanine crystals grown experimentally.

MATERIALS AND METHODS

Materials. L-Alanine and L-leucine were obtained from Sigma-Aldrich. PMMA circular disks were purchased from McMaster-Carr (Elmhurst, IL, USA). Silicon isolator wells (21 wells, 2.0 mm depth × 4.5 mm diameter) were purchased from Grace Biolabs (Bend, OR, USA). Silver target used along with our EMS 150RS sputter coater was acquired from Electron Microscopy Sciences (Hatfield, PA, USA). All aqueous solutions were prepared using deionized water (>18.0 MΩ·cm resistivity at 25 °C) obtained from Millipore Direct Q3 system. All chemicals were used as received.

Methods. *Preparation of Solutions.* The crystallization solution was prepared by dissolving L-alanine solids in a 10 mL vial that contained deionized water (18.2 MΩ·cm) at a concentration of 2.0 M. The solution was then heated at constant temperature of 65 °C. After all the L-alanine was completely dissolved, L-leucine was added to L-alanine solution and investigated using five different experimental conditions as indicated in Table 1.

Crystallization of L-Alanine. This was performed using two different PMMA platforms, (i) silver nanoparticle films deposited-PMMA disk (SNFs-PMMA) and (ii) blank PMMA disk (control surface) [note, PMMA disks were cleaned for 1 min using Harrick plasma cleaner PDC-32G (Ithaca, NY, USA) before use]. One side of the platforms was then covered with a silicon isolator comprised of 21 wells, which afforded us the ability to carry out multiple crystallization experiments. Ten microliters of the prepared L-alanine solutions were placed into the wells on the PMMA and SNFs-PMMA platforms, followed by evaporative crystallization at room temperature and microwave heating. The MA-MAEC technique was carried out using a 900 W Emerson microwave oven (model no. 0009443). Crystals were then grown at room temperature and microwave power level 1 (i.e., duty cycle of 3 s), and optical images of the crystal growth formation were taken.

Characterization. Contact Angle and Surface Tension. Characterization of different platforms was performed using a Kruss Drop Shape Analysis System (DSA) Model Number 10 MK2.

Temperature Measurements. Temperature measurements were carried out using UM14 universal multichannel instrument and Fiso software.

UV−Visible Spectroscopy. SNFs were deposited onto PMMA disks and characterized using a Cary 50 Bio UV−visible spectrophotometer (Varian Inc.).

Optical Microscopy. Images of L-alanine crystal growth were recorded in time intervals using a Swift Digital M10L monocular microscope. The prepared solutions were placed on both platforms [SNFs-PMMA and blank PMMA], in which the growth was observed at 4× focus as solid precipitate using Motic Images 2.0 software.

Raman Spectroscopy and Fourier Transform Infrared Spectroscopy. The iRaman system from B&WTek, Inc. (Newark, DE, USA) and Cary 630 FTIR were used in this work to determine the molecular L-alanine structure.

Powder X-ray Diffraction. PXRD data were obtained using a Rigaku Miniflex PXRD instrument. PXRD data was transferred to and plotted in Sigmaplot 11.

Theoretical Simulations. Theoretical molecular simulations of L-alanine crystals in the presence and absence of L-leucine additive were achieved using Materials Studio software 6.1 (Accelrys Software Inc., San Diego, CA, 2013). It is known that L-alanine crystallizes in an orthorhombic lattice with space group $P2_12_12_1$, and there are four molecules in the unit cell linked by a three-dimensional network of hydrogen bonds. To understand the effects of L-leucine on L-alanine crystals, molecular dynamics simulation with NVT ensemble is carried out using Materials Studio 6.1. The Ewald summation is used for the calculation of long-range interactions. First, CVFF, PCFF, COMPASS, and UNIVERSAL with the force field assigned charges and the equilibration and Gasteiger charge rules are used to optimize the unit

Table 1. Summary of Results for the Crystallization of L-Alanine in the Presence of Increasing Amount of L-Leucine on Blank PMMA Platform and Silver Nanostructured Film Modified PMMA (SNFs-PMMA) Platform at Room Temperature and Using MA-MAEC Technique[a]

sample no.	amino acid weight (wt %)		complete evaporation time, min (size range, μm)				initial crystallization time, min			
			PMMA		SNFs		PMMA		SNFs	
	L-Ala	L-Leu	RT	MW	RT	MW	RT	MW	RT	MW
C1	0.240 g (100%)	0.000 g (0.00%)	170 ± 14 (117–693)	68 ± 6 (159–632)	75 ± 4 (350–572)	23 ± 4 (118–365)	5	5	10	5
C2	0.216 g (91.5%)	0.019 g (8.50%)	117 ± 29 (397–886)	47 ± 2 (352–874)	68 ± 2 (369–1004)	21 ± 2 (309–1023)	5	5	5	5
C3	0.192 g (83.5%)	0.038 g (16.5%)	133 ± 12 (855–1871)	47 ± 6 (96–1997)	65 ± 3 (120–1310)	26 ± 5 (290–1139)	5	5	20	10
C4	0.168 g (74.7%)	0.057 g (25.3%)	245 ± 4 (1832–1887)	72 ± 4 (495–1974)	71 ± 2 (430–1679)	35 ± 2 (666–1425)	180	30	30	10
C5	0.144 g (65.5%)	0.076 g (34.5%)	400 ± 8 (904–1308)	89 ± 6 (582–1839)	226 ± 16 (351–1151)	45 ± 4 (497–2089)	310	50	210	30

[a]RT, room temperature; MW, microwave heating.

cell of L-alanine adopted from Cambridge Structural Database (CSD). The CVFF and the force field assigned charges are used in all the simulations described below.

Once the crystal structure was optimized, the {011} and {120} surfaces of L-alanine were cleaved to a depth of >30 Å and then extended and rebuilt into three-dimensional periodic boxes. The surface dimensions are set >30 Å, and the thickness of vacuum is set to 50 Å to make sure the nonbonding interactions can reach their asymptotic values. Each crystal surface is optimized with a relaxed top layer. Then the effects of L-leucine are studied by molecular dynamics simulations as follows: (i) The likelihood of L-leucine incorporation into L-alanine crystal is assessed by dynamics simulations where one impurity molecule is buried into the rigid and partially relaxed boxes. The incorporation energy of a pure L-alanine molecule in the crystal is calculated for comparison. (ii) Similar to the procedure described by Yang et al., to estimate the effects of L-leucine on flat L-alanine crystal surfaces, a build-in model is employed. In the build-in model, each orientation of L-alanine molecule is substituted by an L-leucine molecule once. Minimization is performed for a proper initial position, which is followed by molecular dynamics simulation. Then molecular dynamics is carried out. During the simulations, the bulk crystal except for the top layer is constrained.

In addition to theoretical simulations above, our experimental PXRD data were imported to Materials Studio 6.1 and the known peaks from the diffraction pattern for our samples were selected to simulate the crystal morphology. More specifically, the imported PXRD data were used to generate a unit cell for L-alanine. A geometry optimization tool was then run using COMPASS for the Forcefield and ultrafine option. Using the morphology module, we generated crystal structures with faces corresponding to the PXRD data. Further modifications to the generated crystal structure were made using the habit module, where the center-to-plane distances of growth faces were modified until they resemble L-alanine crystals grown experimentally. The results of the simulations were compared with the experimentally grown L-alanine crystals with and without L-leucine.

RESULTS AND DISCUSSION

It is important to comment on the choice of L-leucine as an additive for the crystal engineering of L-alanine before introducing the results obtained in this study. It is thought that the similarity of the L-leucine additive to the main molecule allows the additive molecules to add into the crystal lattice and change the natural growth rate of several crystal faces.[18] In this regard, it was previously predicted that L-leucine binds to the crystal surface of L-alanine through weak interactions.[3] Herein, we investigated the effect of L-leucine (pI = 6.04) as an additive in the crystallization of L-alanine (pI = 6.11) on our PMMA platforms.

As shown in Table 1, L-alanine was crystallized using five different experimental conditions, where the mass ratio of L-alanine to L-leucine was as follows: sample C1, 0% w/w; sample C2, 8.50% w/w; sample C3, 16.5% w/w; sample C4, 25.3% w/w; sample C5, 34.5% w/w. At room temperature, for sample C1, the average complete evaporation time of L-alanine on blank PMMA and SNFs-PMMA is 170 ± 14 and 75 ± 4 min and the average crystal size ranges from 117 to 693 μm and from 350 to 572 μm, respectively.[16] With the use of the MA-MAEC technique, the average complete evaporation time was reduced to 68 ± 6 and 23 ± 4 min on blank PMMA and SNFs-PMMA, respectively. The size range of L-alanine crystals on blank PMMA under microwave was 159–692 μm, while SNFs-PMMA had a size range from 118 to 365 μm. We note that sample C1 was used as a control experiment, and the detailed investigation of this experimental condition was described elsewhere.[16] At room temperature, for sample C2, L-alanine solution on blank PMMA and SNFs-PMMA had an average

dx.doi.org/10.1021/cg500204t | Cryst. Growth Des. 2014, 14, 2494–2501

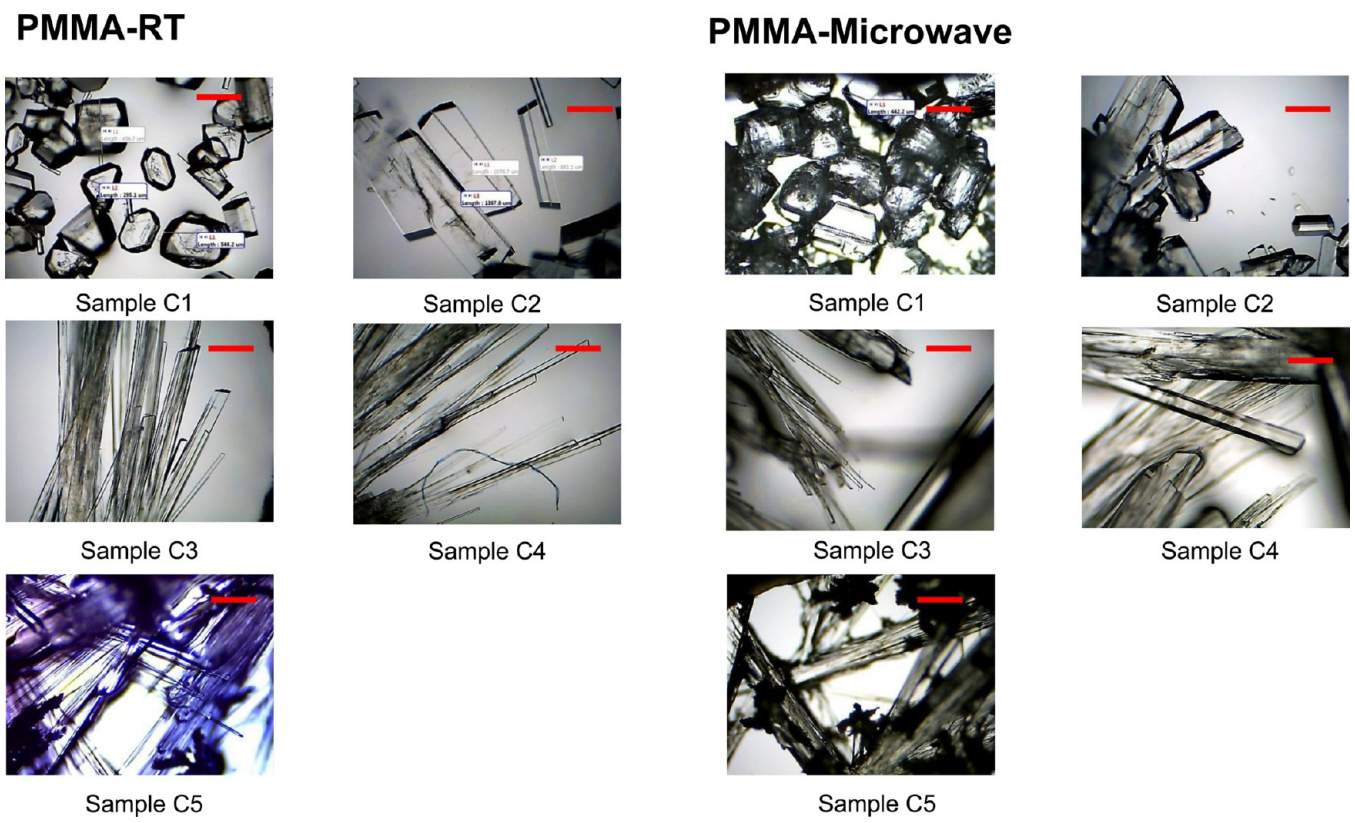

Figure 1. Optical images of L-alanine crystals formed on PMMA platform at room temperature and using microwave heating (Samples C1−C5). Scale bar =5 00 μm.

complete evaporation time of 117 ± 29 and 68 ± 2 min and an average size range of 397−886 and 309−1023 μm, respectively. Using the MA-MAEC technique, the average complete evaporation times on blank PMMA and SNFs-PMMA were 47 ± 2 and 21 ± 2 min, respectively. The average size ranges on blank PMMA and SNFs-PMMA were 352−874 and 309−1023 μm, respectively. Similar results, a reduction in complete evaporation time and an increase in crystal size, were obtained for samples C3, C4, and C5 and are shown in Table 1. The complete information on the size and number of crystals grown from all samples on blank PMMA and SNFs-PMMA at room temperature and using the MA-MAEC technique is provided in Figures S3 and S4 (Supporting Information)

It is interesting to note that the increase in the L-leucine concentration in the initial L-alanine/L-leucine mixture resulted in an increase in the total evaporation time for experiments carried out both at room temperature and using the MA-MAEC technique. In addition, there is a systematic increase in the size of the L-alanine crystals grown on SNFs-PMMA using the MA-MAEC technique unlike other experimental conditions (RT and MW, see Table 1, where there is no significant increase in the size of L-alanine crystals after sample C3). These results can be attributed to the presence of L-leucine additive, which is thought to slow down the growth rate of L-alanine crystals. Direct evidence for this hypothesis is provided in Table 1, which shows that the appearance of initial L-alanine crystals (i.e., initial crystallization time) occurred at increasingly delayed times as the initial concentration of L-leucine was increased. [Note, initial crystallization is the time at which the first crystal visually was detectable with our microscope during the crystallization process]. In this regard, the initial L-alanine crystals appeared within 5−10 min of the start of the crystallization experiments for L-alanine solutions with no or small amounts (samples C1 to C3) on both blank PMMA and SNFs-PMMA at room temperature and using the MA-MAEC technique. At room temperature, the initial L-alanine crystals for samples C4 and C5 on blank PMMA were observed at 180 and 310 min, respectively. On SNFs-PMMA, the appearance of L-alanine crystals at room temperature was relatively faster (30 and 210 min for samples C4 and C5) than those observed on blank PMMA, which can be attributed to the benefit of using silver nanostructures as selective nucleation sites. The advantage of using the MA-MAEC technique in the rapid crystallization of L-alanine with L-leucine became more evident as the initial crystallization times were reduced to 30 min (for sample C5, SNFs-PMMA, MW), which is 10-fold faster than that observed for sample C5 on blank PMMA at room temperature.

Optical microscopy was employed to ascertain the change in morphology of L-alanine crystals grown in the absence and presence of increasing amounts of L-leucine additive on blank PMMA at room temperature and using microwave heating for samples C1−C5, and these optical images are shown in Figure 1. We note that these images were taken after the complete evaporation of the solvent to demonstrate the crystal quality at the end of the experiment. One can harvest the grown crystals at any time simply by removing the solvent. As demonstrated before, L-alanine crystals grown from sample 1 (control experiment, which contains no additive) at both room temperature and microwave heating have their typical tetragonal shape. With the addition of a small amount of L-leucine to the initial L-alanine solution, that is, sample C2, the morphology of L-alanine crystals is slightly modified to an elongated plate like crystal structure; this was observed for both

dx.doi.org/10.1021/cg500204t | Cryst. Growth Des. 2014, 14, 2494−2501

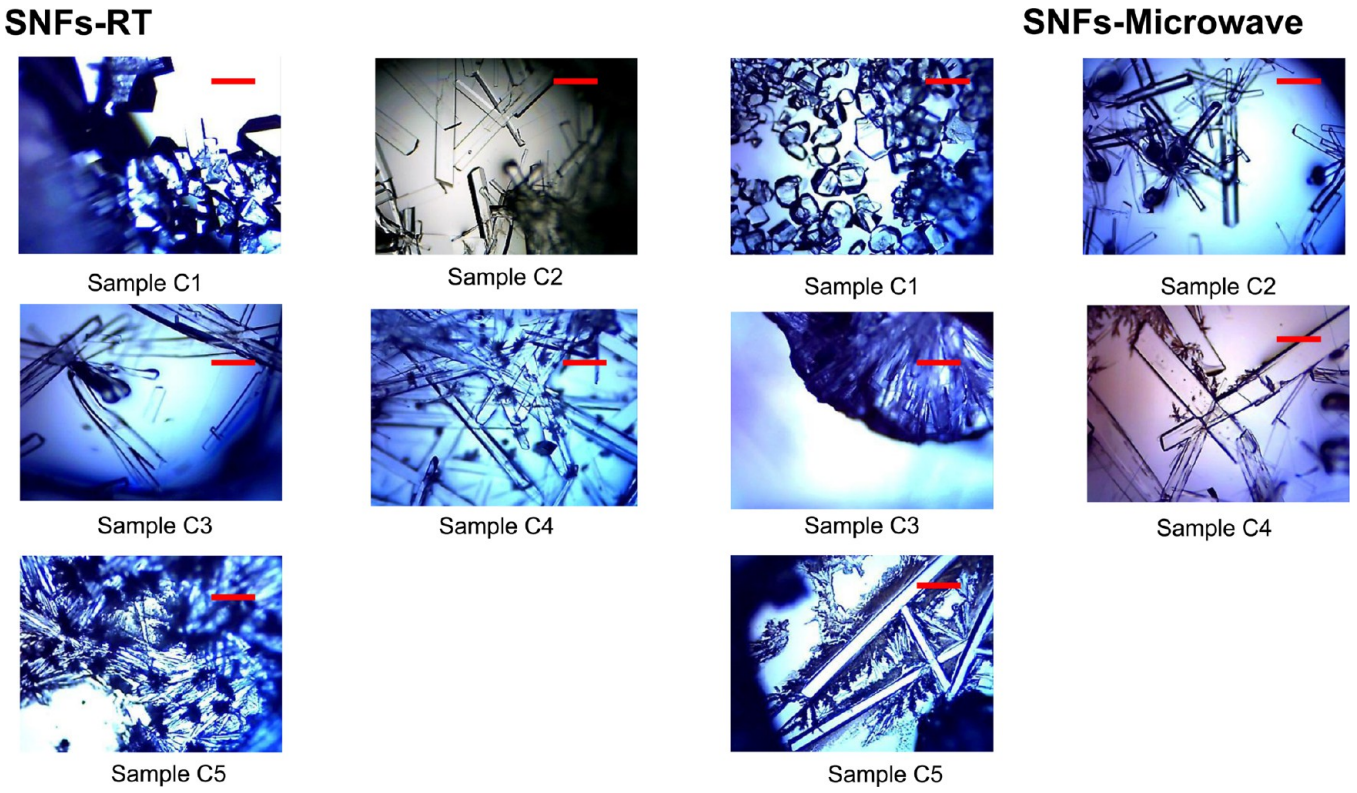

Figure 2. Optical images L-alanine crystals formed on SNFs-PMMA platform at room temperature and using the MA-MAEC technique (samples C1−C5). Scale bar = 500 μm.

room temperature and microwave heating conditions. As the initial amount of L-leucine is increased (for samples C3−C5), the shape of L-alanine crystals grown at room temperature and using microwave heating appears to get thinner and longer.

In order to study the effect of L-leucine on L-alanine crystals using the MA-MAEC technique, optical images of L-alanine crystals grown on SNFs-PMMA at room temperature and using MA-MAEC are shown in Figure 2. The change in morphology of L-alanine with addition of a small amount L-leucine (i.e, sample C2) appears to have a greater effect using SNFs-PMMA than using blank PMMA. It is apparent that L-alanine crystals grown on SNFs-PMMA from sample C2 both at room temperature and using MA-MAEC resemble the wire-like structure seen only in samples C3−C5 on blank PMMA, where crystals grown on blank PMMA from sample C2 were not as elongated (Figure 1). The difference between morphologies of L-alanine crystals grown from sample C2 on blank PMMA and SNFs-PMMA implies that silver nanostructures further promote the adsorption of L-leucine onto the crystal surface of L-alanine by accelerating the crystallization process [note, Table 1 shows a shorter evaporation time using SNFs-PMMA]. In addition, the length of the L-alanine crystals grown from samples C3−C5 using MA-MAEC technique continued to increase and reached a maximum length of ∼2 mm as the solvent was completely evaporated. We predict that the growth of longer L-alanine crystals is possible using our crystallization platforms provided that the initial L-alanine/L-leucine mixture is still available for crystal growth, which can be accomplished by addition of the initial mixture intermittently as the solvent evaporates (i.e., semibatch mode). The use of semibatch mode is beyond the scope of this work and will be reported elsewhere.

In addition to the benefits of using the MA-MAEC technique described above, one can use our technique to harvest L-alanine crystals with desired shape and size before the complete evaporation of the solvent. To demonstrate this utility, the growth of L-alanine crystals from sample C4 on SNFs-PMMA at room temperature and using MA-MAEC was followed by optical microscopy and is shown in Figure 3. In addition, the size and the growth rate of L-alanine crystals (circled in the figure) were calculated and are shown in Figure S5 (Supporting Information). The growth rate (shown as bars in Figure S5) for L-alanine crystals grown at room temperature initially increases from 60 to 90 μm/min for 10 min, followed by a rate of 45−55 μm/min for 20 min, and slows significantly to <15 μm/min in the last 10 min before the complete evaporation of the solvent. The size of the L-alanine crystals increases significantly during the fast and the constant growth rate periods and levels off at the end of the experiment (due to lack of solvent, L-alanine, and L-leucine). Under the MA-MAEC technique, both the crystal size and the growth rate of the L-alanine crystals display an exponential increase until the complete evaporation of the solvent (up to 200 μm/min in 15 min), which implies that the growth of L-alanine crystals can potentially be continued depending on the availability of additional L-alanine/L-leucine mixture.

The characterization of L-alanine crystals was undertaken by PXRD measurements and FT-IR and Raman spectroscopy. Figure 4 shows the PXRD patterns of L-alanine crystals grown from samples C1−C5 using the MA-MAEC technique (see Figure S9 in Supporting Information for other experimental conditions). The intensities for L-alanine crystals grown from all samples appear in the same diffraction planes.[16] PXRD studies reveal that there are no discernible differences in the diffraction patterns obtained from all samples, which implies that the

dx.doi.org/10.1021/cg500204t | Cryst. Growth Des. 2014, 14, 2494−2501

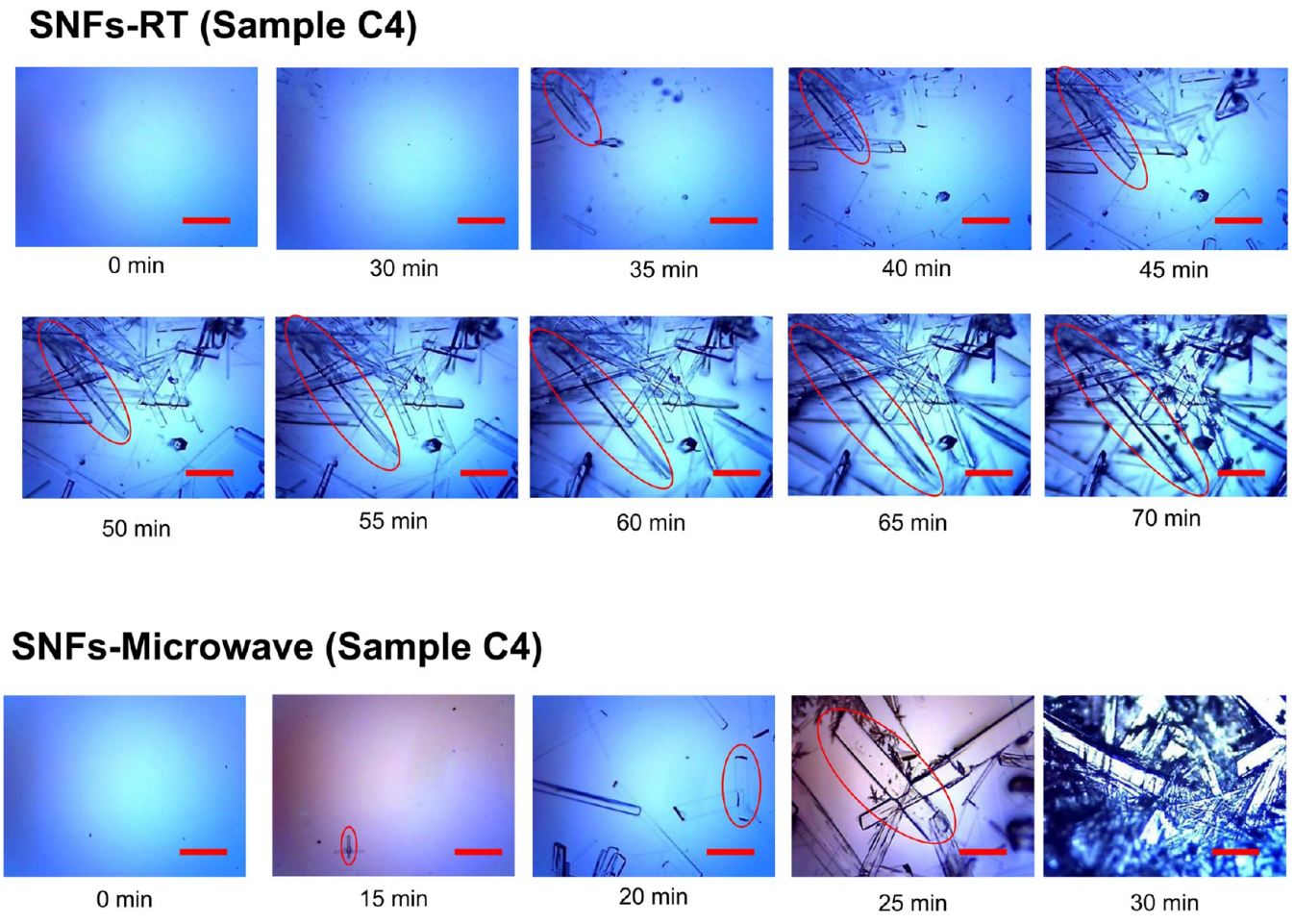

Figure 3. Time progression of the growth of L-alanine crystals on SNFs-PMMA platform at room temperature and using the MA-MAEC technique (sample C4). Scale bar = 500 μm.

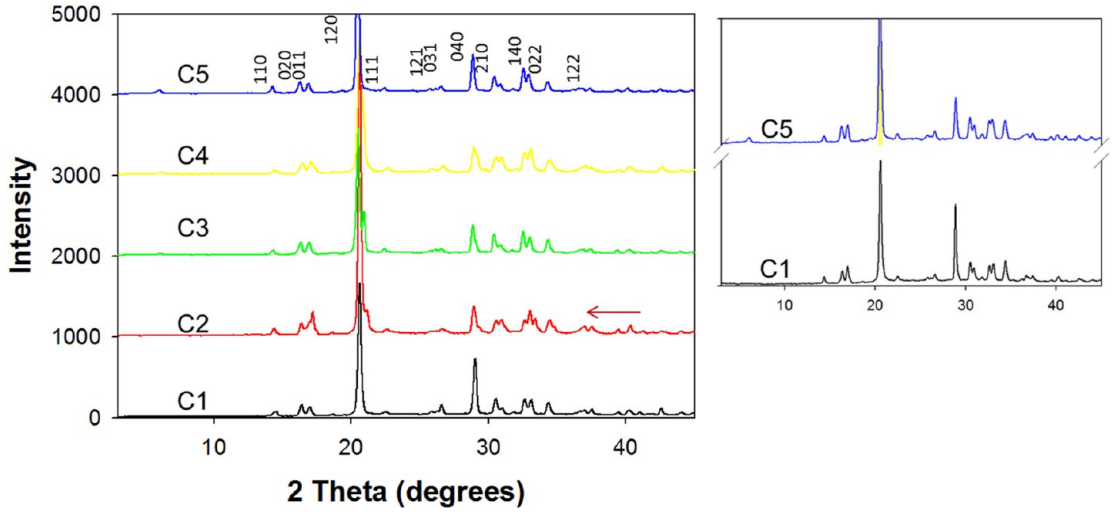

Figure 4. PXRD data for L-alanine crystal on SNFs-PMMA platform using the MA-MAEC technique (samples C1−C5).

observed morphological changes occurred with crystals faces common to all samples. This observation was corroborated by Raman and FT-IR measurements (Figures S6−S8, Supporting Information). Both methods of vibrational analysis revealed that all peaks for L-alanine crystals grown from all samples occur at the identical positions, despite the differences in the crystal morphology. This observation can be attributed to the structural similarities in terms of type of chemical bonds between L-alanine and L-leucine.

It was previously reported that the morphological differences between L-alanine with no additive and with L-leucine additive may be due to the additive selectively adsorbing to the {120} face of L-alanine via hydrophobic interactions. The {120} faces are formed along the channels created by hydrogen bonding

dx.doi.org/10.1021/cg500204t | *Cryst. Growth Des.* 2014, 14, 2494−2501

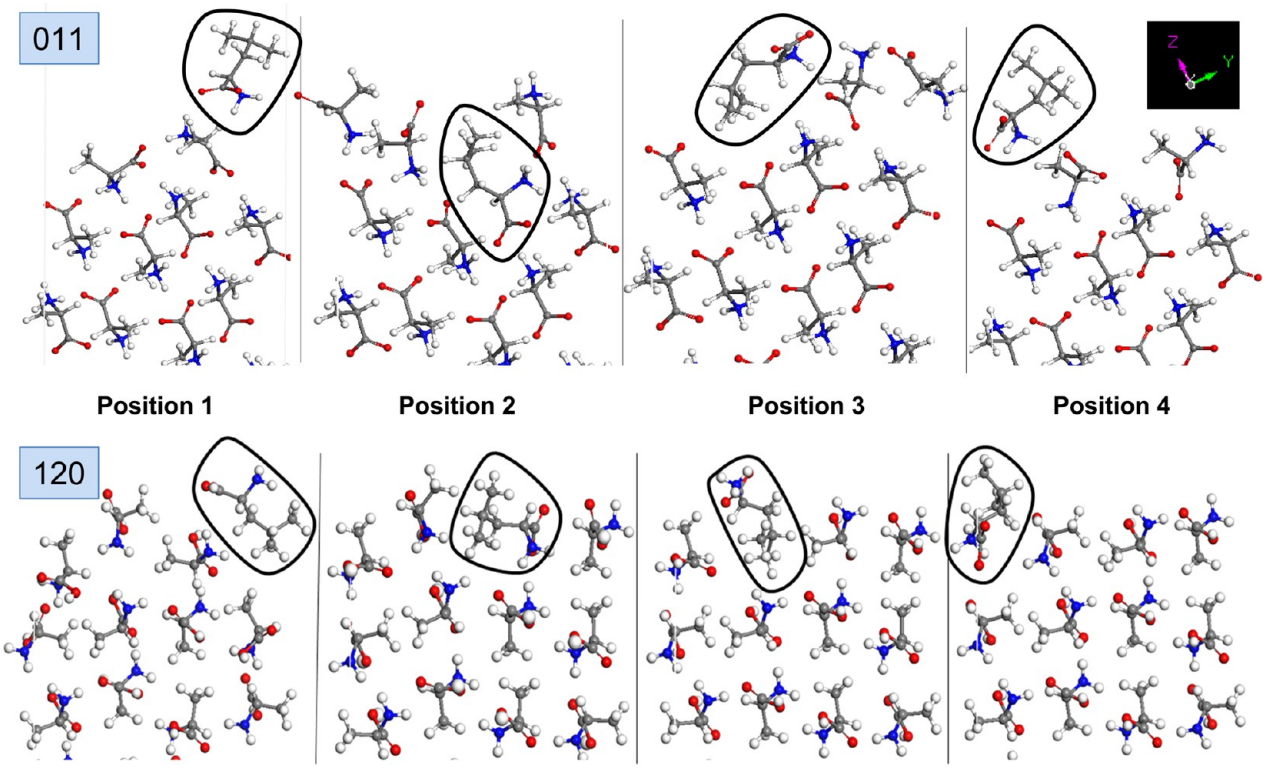

Figure 5. Simulated L-alanine surfaces: (top) {011} and (bottom) {120} substituted by L-leucine on four symmetry positions in the build-in model. L-leucine molecule is circled.

where the methyl functional groups are present, thus making the faces naturally hydrophobic. The dissimilar isopropyl functional group of L-leucine binds with the activated α carbon of one of the methyl groups found in the {120} face and, as a result, reduces the face's growth rate but has no effect on the growth rate of the faces perpendicular to it, such as {110} and {210}. These faces perpendicular to the {120} face are comprised of mainly amine and carboxylic groups, rendering them hydrophilic in nature. Subsequently, we have employed the classical build-in model, which is widely used for estimating the impurity effects, to study the effect of L-leucine on flat interface of L-alanine.

In this regard, the build-in model is used to predict the effect of L-leucine by calculating the surface energies ($E_{surface}$) when one L-alanine molecule on the surface is substituted by one L-leucine molecule. Since four different orientations of L-alanine molecules are possible on {011} and {120} interfaces, the calculations on each surface are repeated for all possible orientations as shown in Figure 5. For both {011} and {120}, the presence of substituted L-leucine results in the disruption of the arrangement of L-alanine molecules, which are rearranged in a fashion to lower the repulsive energy. Subsequently, the incorporation of L-leucine molecules into L-alanine results in an increase in the total surface energies for some positions of L-leucine (positions 1, 2, and 3 for {011}, position 1 for {120}; Table 2), which indicates a reduction in the growth rate (i.e., inhibition). As shown in Table 2, the surface energy for {011} with and without L-leucine is significantly lower than that for {120} in all five cases. This implies that the relative growth rate of {011} is significantly faster than {120}. On the other hand, our calculations show a decrease in surface energy in position 4 for {011} and positions 2 and 3 for {120}, which indicates an increase in the growth rate when L-leucine is substituted in these positions. For {120}, L-leucine is more easily incorporated into position 3 than position 2, where the most dominant growth of {120} is predicted to takes place. The comparison of $\Delta E_{surface}$ values can be used to determine the positions where the incorporation of L-leucine results in the highest inhibition of growth rate. For example, the incorporation of L-leucine into position 2 in {011} results in a higher inhibition of growth rate than that at positions 1 and 3. In addition, for {120}, the incorporation of L-leucine into position 1 results in further increase in the surface energy, where the growth rate of {120} is inhibited. We note that our calculations for the incorporation of L-leucine in position 4 for {120} did not yield stable crystals, which implies that L-leucine cannot be incorporated into L-alanine crystal from this position. To further expand our knowledge on the crystallization of L-alanine using other additives to create amino acid crystals with desired shapes for nonlinear optical applications, we intend to investigate the effects of multiple additives, such as L-threonine, L-glutamine,

Table 2. Surface Energies L-Leucine Substituted L-Alanine Surfaces in the Build-in Model

crystal face	L-leucine's position	total enthalpy (kcal/mol)	$\Delta E_{surface}$ ($E_{position} - E_{pure}$)
{011}	pure	−2644.4	0.0
	1	−2643.7	0.7
	2	−2620.3	24.1
	3	−2636.5	7.9
	4	−2646.3	−1.9
{120}	pure	−87.5	0.0
	1	−84.0	3.5
	2	−89.8	−2.3
	3	−186.6	−99.0
	4	Not determined	Not determined

dx.doi.org/10.1021/cg500204t | Cryst. Growth Des. 2014, 14, 2494−2501

and L-methionine at once on the morphology of L-alanine using the MA-MEAC technique. These results will be reported in due course.

CONCLUSIONS

Crystallization of L-alanine using the MA-MAEC technique was carried out at a rapid rate (up to 10-fold faster than at room temperature) both in the presence and in the absence of L-leucine additive. Optical microscopy measurements revealed that the presence of L-leucine resulted in a systematic increase in the size and change in the shape of L-alanine. FTIR and Raman spectroscopy measurements did not yield discernible results between different experimental conditions to investigate the effect of L-leucine on the growth of L-alanine, which was attributed to the similar molecular structures of both molecules. PXRD data were used in conjunction with theoretical calculations to identify the faces of L-alanine crystals grown from all samples. Further theoretical simulations showed that the surface energy for {011} was significantly lower than that for {120}, which implied that the relative growth rate of {011} was faster than that of {120}. In addition, we were able to predict surface energy values when L-leucine was incorporated into L-alanine crystals in four possible positions. These predictions revealed that the inhibition of the growth rate of {120} occurs due to the incorporation of L-leucine in position 1, while the incorporation of L-leucine in the other two positions results in an increase in the growth rate of {120}. In addition, the theoretical simulations predicted that the growth rate of {011} can be partially inhibited when L-leucine is incorporated into three different positions on the L-alanine crystals.

ASSOCIATED CONTENT

Supporting Information

Additional information related to the characterization of SNFs, actual temperature measurements on the PMMA platforms, FTIR, Raman, and PXRD data, and results of additional theoretical simulations. This material is available free of charge via the Internet at http://pubs.acs.org.

AUTHOR INFORMATION

Corresponding Author

*Corresponding author: Kadir.Aslan@morgan.edu.

Notes

The authors declare no competing financial interest.

ACKNOWLEDGMENTS

The project described was supported by Maryland Innovation Initiative (Phase 1) Award from Technology Development Corporation. Additional partial support was provided by Award Number 5-K25EB007565-05 from the National Institute of Biomedical Imaging and Bioengineering. The content is solely the responsibility of the authors and does not necessarily represent the official views of the National Institute of Biomedical Imaging and Bioengineering or the National Institutes of Health. Additional financial support was provided by NIH MARC U* STAR program (Grant No. 5T34GM007977-27).

REFERENCES

(1) Tiekink, E. R., Zukerman-Schpector, J., Eds. *The importance of PI-interactions in crystal engineering: Frontiers in crystal engineering*; Wiley: Chichester, U.K., 2012.

(2) Mirza, S.; Miroshnyk, I.; Heinämäki, J.; Antikainen, O.; Rantanen, J.; Vuorela, P.; Vuorela, H.; Yliruusi, J. Crystal morphology engineering of pharmaceutical solids: Tabletting performance enhancement. *AAPS PharmSciTech* **2009**, *10* (1), 113−119.

(3) Lechuga-Ballesteros, D.; Rodríguez-Hornedo, N. The relation between adsorption of additives and crystal growth rate of L-alanine. *J. Colloid Interface Sci.* **1993**, *157* (1), 147−153.

(4) Lechuga-Ballesteros, D.; Rodriguez-Hornedo, N. Growth and morphology of L-alanine crystals: Influence of additive adsorption. *Pharm. Res.* **1993**, *10* (7), 1008−1014.

(5) Doki, N.; Yokota, M.; Sasaki, S.; Kubota, N. Simultaneous crystallization of D-and L-asparagines in the presence of a tailor-made additive by natural cooling combined with pulse heating. *Cryst. Growth Des.* **2004**, *4* (6), 1359−1363.

(6) Schulz, G. E.; Schirmer, R. H. *Principles of protein structure*; Springer-Verlag KG: New York, 1979.

(7) Derbel, N.; Hernández, B.; Pflüger, F.; Liquier, J.; Geinguenaud, F.; Jaïdane, N.; Ben Lakhdar, Z.; Ghomi, M. Vibrational analysis of amino acids and short peptides in hydrated media. I. L-glycine and L-leucine. *J. Phys. Chem. B* **2007**, *111* (6), 1470−1477.

(8) Raj, S. G.; Kumar, G. R. Structural and hardness of nonlinear optical L-alanine single crystals. *Adv. Mater. Lett.* **2011**, *2* (3), 176−182.

(9) Lechuga-Ballesteros, D.; Rodríguez-Hornedo, N. Effects of molecular structure and growth kinetics on the morphology of L-alanine crystals. *Int. J. Pharm.* **1995**, *115* (2), 151−160.

(10) Lechuga-Ballesteros, D.; Rodríguez-Hornedo, N. The influence of additives on the growth kinetics and mechanism of L-alanine crystals. *Int. J. Pharm.* **1995**, *115* (2), 139−149.

(11) Yang, X.; Qian, G.; Duan, X.; Zhou, X. Effect of impurity on the lateral crystal growth of L-alanine: A combined simulation and experimental study. *Ind. Eng. Chem. Res.* **2012**, *51* (45), 14845−14849.

(12) Alabanza, A. M.; Aslan, K. Metal-assisted and microwave-accelerated evaporative crystallization: Application to L-alanine. *Cryst Growth Des* **2011**, *11* (10), 4300−4304.

(13) Pinard, M. A.; Aslan, K. Metal-assisted and microwave-accelerated evaporative crystallization. *Cryst Growth Des* **2010**, *10* (11), 4706−4709.

(14) Pinard, M. A.; Grell, T. A. J.; Pettis, D.; Mohammed, M.; Aslan, K. Rapid crystallization of L-arginine acetate on engineered surfaces using metal-assisted and microwave-accelerated evaporative crystallization. *CrystEngComm* **2012**, *14* (14), 4557−4561.

(15) Mohammed, M.; Syed, M. F.; Bhatt, M. J.; Hoffman, E. J.; Aslan, K. Rapid and selective crystallization of acetaminophen using metal-assisted and microwave-accelerated evaporative crystallization. *Nano Biomed. Eng.* **2012**, *4* (1), 35−40.

(16) Alabanza, A. M.; Mohammed, M.; Aslan, K. Crystallization of L-alanine in the presence of additives on a circular PMMA platform designed for metal-assisted and microwave-accelerated evaporative crystallization. *CrystEngComm* **2012**, *14* (24), 8424−8431.

(17) Aslan, K.; Geddes, C. D. Microwave-accelerated metal-enhanced fluorescence: platform technology for ultrafast and ultrabright assays. *Anal. Chem.* **2005**, *77* (24), 8057−8067.

(18) Lahav, M. L.; Leiserowitz, L. Tailor-made auxiliaries for the control of nucleation, growth and dissolution of two- and three-dimensional crystals. *J. Phys. D: Appl. Phys.* **1993**, *26*, B22−B31.